Available online at www.sciencedirect.com
SCIENCE DIRECT®
Earth and Planetary Science Letters 246 (2006) 70–89
EPSL
www.elsevier.com/locate/epsl

Chemical and carbon isotopic fractionations of gaseous hydrocarbons during abiogenic oxidation

Changchun Pan *, Linping Yu, Jinzhong Liu, Jiamo Fu

State Key Laboratory of Organic Geochemistry, Guangzhou Institute of Geochemistry, Chinese Academy of Sciences, Wushan, Guangzhou 510640, P.R. China

Received 15 January 2006; received in revised form 30 March 2006; accepted 8 April 2006
Available online 19 May 2006
Editor: C.P. Jaupart

Abstract

The variations of chemical and carbon isotopic compositions in gaseous hydrocarbons upon abiogenic oxidation by sulfates, hematite and both in laboratory studies were clearly demonstrated through a unique two-step experimental approach. In the first step, a large number of small gold capsules containing gaseous hydrocarbons were prepared by kerogen pyrolysis experiments, which were conducted under the same condition (450 °C and 50 MPa for 72 h) using the same kerogen. The analytical results demonstrated that the chemical and carbon isotopic compositions of gases were almost identical among the capsules. In the second step, each of these gaseous hydrocarbon-bearing capsules, along with mineral oxidant (hematite, or magnesium sulfate heptahydrate, or both) and deionized water (15% of the amount of the oxidant), was placed into a large gold capsule. After welding (sealing), the small gaseous hydrocarbon-bearing capsule was forced to leak while the large capsule remained undamaged by compressing the large capsule from the outside at the position where this small capsule was located. Then, these large capsules containing gas and mineral reactants were heated isothermally at 350 °C and 50 MPa for 72, 144, 216 and 288 h, respectively. The results of the oxidation experiments with increasing heating time can be outlined as follows: (1) the amount of methane remained almost unchanged in the experiments using hematite and the mixed oxidants (hematite+$MgSO_4$) while it increased substantially in the experiment using $MgSO_4$ after 72 h, indicating methane was one of the final products of C_{2+} oxidation; (2) the amounts of C_2–C_5 hydrocarbons decreased consistently and more rapidly in the experiment using $MgSO_4$ than that using hematite and the mixed oxidants; (3) the oxidation rates of gas hydrocarbons increased with increasing carbon number of hydrocarbons; (4) the oxidation rates of *i*-butane and *i*-pentane were substantially higher than those of the corresponding *n*-butane and *n*-pentane; (5) the amount of H_2S increased substantially in the experiment using $MgSO_4$, whereas it was below the detection level in the experiments using hematite and the mixed oxidants; (6) the $\delta^{13}C$ values of C_1–C_5 hydrocarbons became less negative and the isotopic fractionation extent increased with increasing carbon number of hydrocarbons and oxidation extent; (7) carbon isotopic fractionation factor α (k^{12}/k^{13}) decreased with increasing oxidation rate of gas hydrocarbons; and (8) the rate of thermochemical sulfate reduction (TSR) was strongly dependent upon the presence and concentrations of H_2S.

Keywords: abiogenic oxidation; gaseous hydrocarbons; themochemical sulfate reduction (TSR)

* Corresponding author.
E-mail address: cpan@gig.ac.cn (C. Pan).

0012-821X/$ - see front matter © 2006 Elsevier B.V. All rights reserved.
doi:10.1016/j.epsl.2006.04.013

1. Introduction

Numerous studies have documented the oxidation of gaseous hydrocarbons in carbonate reservoirs through thermochemical sulfate reduction (TSR) [1–19]. The overall process can be represented by the general reaction [13,20]:

$$CaSO_4 + \text{hydrocarbon gases} \rightarrow CaCO_3 + H_2S + H_2O \pm S \pm CO_2$$

The notorious result of TSR is that the amount of H_2S increases substantially in gas hydrocarbon reservoirs [1–19]. Gas hydrocarbons can be also oxidized by hematite, magnetite and other ferric (Fe^{3+})-bearing minerals [20,21]. Surdam et al. demonstrated that hydrocarbon invasion resulted in bleaching and porosity enhancement of red sandstones [22]. This phenomenon was interpreted as follows: (1) hematite in red sandstones was reduced by hydrocarbons, resulting in color bleaching; (2) hydrocarbons were oxidized into carboxylic acids which dissolved the carbonate cements [22]. Previous studies also indicated that carboxylic acids widely occur in oilfield brines at concentrations up to 10,000 ppm [23–26]. Franks and Forester demonstrated that the isotopic composition of carbons in carbonated cements in the U.S. Gulf Coast decreases systematically ($\delta^{13}C$ values of as low as −16‰) with increasing temperatures (up to 200 °C) [26]. Seewald regarded these data (the abundances of carboxylic acids and $\delta^{13}C$ values of carbonated cements) as strong evidences of pervasive hydrocarbon oxidation by hematite, magnetite and other ferric (Fe^{3+})-bearing minerals in petroleum-producing sedimentary basins [20].

In comparison with field measurements, laboratory studies have been scarce. Kiyosu and Krouse [27] conducted an experimental study on the reaction of flowing methane with CuO or hematite and found that the produced CO_2 was more depleted in ^{13}C than the reactant methane. Their experiments were performed at high temperatures (400–650 °C), under atmospheric pressure, and in the absence of water, conditions strikingly different from those in sedimentary basins. Seewald [21] performed an extensive experimental study on oxidation of low-molecular-weight aqueous hydrocarbons in mineral buffered redox systems (pyrite–pyrrhotite–magnetite, hematite–magnetite–pyrite and hematite–magnetite) at 300–350 °C and 350 bar, and the results revealed that the decomposition of aqueous *n*-alkanes proceeds through a sequence of oxidation and hydration reactions that sequentially produce alkenes, alcohols, ketones, and organic acids as the reaction intermediates. Organic acids subsequently undergo decarboxylation and/or oxidation reactions to form CO_2 and methane or shorter chain saturated hydrocarbons [21]. However, no carbon isotopic data were obtained due to the low abundances of alkanes employed in the experimental systems. Several experimental studies on TSR have been also reported using organic matter soluble in water, such as acetic acid, other than hydrocarbons [28–31]. These studies mainly focused on the TSR rate, rather than the fractionation of gaseous hydrocarbons in both the chemical and isotopic compositions [28–31]. To date, the phenomenon of TSR has mainly been observed in gas hydrocarbon reservoirs in sedimentary basins [1–19]. However, experimental work on the reaction between sulfates and gas hydrocarbons has been rarely reported. The first aim of the present study was to simulate the oxidation of gas hydrocarbons through TSR in laboratory. A successful laboratory simulation can greatly improve our understanding of the TSR process in natural environments and enhance our ability to predict H_2S concentrations in gas reservoirs in sedimentary basins.

The chemical and carbon isotopic data of gas hydrocarbons have been used as a critical indication to differentiate gas hydrocarbon origins (i.e., bacterial or thermogenic), sources (kerogen characteristics), generative manners (directly cracked from kerogen, or secondarily cracked from oil), thermal maturation levels, and filling histories of reservoirs (accumulative or instantaneous) [32–41]. The chemical and isotopic variations of gas hydrocarbons after entering the reservoirs were ignored in these previous studies [32–41]. If the reaction between gas hydrocarbons and Fe^{3+}-bearing minerals occur widely in natural systems, just as Seewald suggested [20,21], the chemical and isotopic fractionations of gas hydrocarbons created by this reaction need to be considered seriously. So far, no field study has been reported that deals with this problem. The second aim of the present study was to investigate the chemical and carbon isotopic variations of gas hydrocarbons during oxidation by hematite, sulfates and both of them in experimental systems, which could improve our understanding of the origins and evolution of gas hydrocarbons in sedimentary basins.

2. Experimental

Our experiments were performed in a chemically inert environment (gold capsule) using hydrocarbon reactants comparable to those of gas hydrocarbon reservoirs in sedimentary basins. In order to investigate the chemical and isotopic variations of gas hydrocarbons in the oxidation experiments, we need to place a natural gas sample, whose chemical and isotopic compositions are known, into the reaction cells without any changes during the whole performance process prior to heating. It is impossible to inject a natural gas sample directly to the cells due to the extremely

evaporative nature of the gas components (esp. methane). Therefore, a unique two-step experimental approach was adopted in the present study. The first step was to prepare a large number of small capsules containing gaseous hydrocarbons comparable to those in natural reservoirs. The chemical and isotopic compositions of the gas components were "identical" among these capsules. The second step was to perform the oxidation experiments using the gas components within the prepared capsules as the reactants.

2.1. Preparation of "identical" gas hydrocarbon-bearing gold capsules

This is the critical step for the entire experimental work. Sixty small gold capsules (3 mm in outside diameter, 0.20 mm in wall thickness and 30 mm in length) were welded at one end before being loaded with samples. About 18 mg of kerogen was placed into each capsule, which was separated from the Estonian Ordovician immature oil shale (kukersite). This kerogen had been stored in refrigerator for 3 yr prior to use in pyrolysing experiments in the present study. The contents of organic carbon, hydrogen, oxygen and nitrogen of this kerogen are 67.02%, 8.26%, 14.90% and 3.00%, respectively, measured just before the pyrolysing experiment using an Elementar vario EL III. In comparison with the composition of kukersite kerogen reported by Derenne et al., i.e., 67.0% C, 8.3% H, 12.8% O, 2.2% N and 3.5% S [42], the oxygen content of our kerogen sample is relatively high, possibly due to partial oxidation during storage [43]. This kerogen was used in the present study with the consideration that it could generate a large amount of gas hydrocarbons with less pyrobitumen residues. Once loaded, the open end of each capsule was purged with Ar before being squeezed in a vise to create an initial seal, which was subsequently welded in the presence of Ar. During welding, the previously welded end was submerged in cold water to prevent heating of the reactants. Then, these gold capsules were placed into 10 steel pressure vessels, with six capsules in one vessel. These vessels were previously filled with water and connected to each other with pipelines. Therefore, the internal pressure within all the vessels was identical and adjusted to 50 MPa by pumping water in and out of the vessels. The uncertainty of the pressure was <0.1 MPa. Our experimental system permitted all the 10 pressurized vessels to be placed in a single furnace. A fan was installed at the bottom of the furnace to keep the vessels inside under the same temperature conditions during the experiment. The temperature of the vessels was raised to 450 °C within 10 h and held for 72 h. The uncertainty of the temperature was $<\pm 1$ °C. After heating, the vessels were quenched to room temperature in cold water within 10 min. During quenching, the pressure was held at 50 MPa to prevent the capsules from leaking. After cooling, the pressure inside the vessel was gradually reduced to the atmospheric pressure. Nine of the above capsules from different vessels were selected for the chemical and isotopic compositional analyses of the volatile pyrolysates. Another capsule was taken for the analysis of large pyrolysates.

2.2. Laboratory simulation on the biogenic oxidation of gas hydrocarbons

Gas components in the small gold capsules prepared with the above-mentioned procedures were used as the initial reactants. Each of the remaining gas hydrocarbon-bearing capsules, along with mineral oxidants (700 mg hematite, or 600 mg magnesium sulfate heptahydrate, or 350 mg hematite plus 300 mg magnesium sulfate heptahydrate) and 100 mg deionized water, were placed into a large gold capsule (6 mm in outside diameter, 0.25 mm in wall thickness and 60 mm in length). Although anhydrite appears to be the reactive oxidant and is replaced by calcite and dolomite in natural TSR reservoirs [1–19], it is generally not used in laboratory TSR studies due to its low solubility [28–31]. Magnesium (Mg^{2+}) is always present in natural TSR reservoirs and may play a catalytic role in natural TSR processes (Yongchun Tang, personal communication). Therefore, magnesium sulfate ($MgSO_4 \cdot 7H_2O$) was used in the present study. After the large capsule was welded (sealed), the small gas hydrocarbon-bearing capsule was forced to leak while the large capsule was maintained undamaged by compressing the large capsule from the outside at the position where this small capsule was located. Therefore, the gas components could be in contact with the mineral oxidants. Three of these large capsules were tested. The results indicated that the small gold capsule inside was leaked in all cases upon compressing. The kerogen residues and large released pyrolysates (polynuclear aromatics) could also react with the oxidants, resulting in the release of some gas components. The nine small capsules aforementioned, which had been pierced for the analyses of the volatile products, were used for the comparative experiments. Each of these nine capsules plus mineral oxidants (700 mg hematite, or 600 mg magnesium sulfate heptahydrate, or 350 mg hematite plus 300 mg magnesium sulfate heptahydrate) and 100 mg deionized water were placed into a large gold capsule. These large capsules without the initial gas reactants were heated together with those containing gas reactants. The experiments were conducted using the same apparatus for the kerogen pyrolysing as described above. Two large capsules were placed into one vessel. Ten vessels were used for the same run. The internal pressure of all the vessels was maintained

at 50 MPa. The temperature of the vessels for four runs were increased to 350 °C in 10 h and held for 72, 144, 216 and 288 h, respectively. After oxidation experiments, the chemical and isotopic compositions of the gas components in the large capsules were analyzed with the same procedures as those for the initial gas components in the nine small capsules.

2.3. Chemical and isotopic analyses

The volatile components in the capsules were collected and concentrated in a special device connected with an Agilent 6890 N GC modified by WassonECE Instrumentation (Fig. 1). Initially, valve D was closed while valves A, B and C were open. The whole device was evacuated by a vacuum pump to reach an internal pressure of less than 1×10^{-2} Pa. Valves A, B and C were closed, and valve D was open to allow the standard gases to get into the space entrapped within valves A, B and D, with a volume 30.6 ml. Once valve D was closed, the amount of the standard gases can be determined by the pressure gauge. Valve B was open to allow gases to get into the 6890N GC, through which the GC analyses of both the organic and inorganic gas components were performed in an automatically controlled procedure. This modified GC is equipped with seven valves, eight columns and three detectors, i.e., an FID for analyzing gas hydrocarbons (helium as a carrier gas), a TCD for analyzing H_2 (nitrogen as a carrier gas) and another TCD for analyzing the other inorganic gases (helium as a carrier gas). The oven temperature for the hydrocarbon gas analysis was initially held at 70 °C for 6 min, ramped from 70 to 130 °C at 15 °C/min, from 130 to 180 °C at 25 °C/min, and then held at 180 °C for 4 min, whereas it was held at 90 °C for the inorganic gas analysis. The analysis of all gases was carried out by one single injection. An equation between the amounts and the values of FID and TCD responses for the gas components were obtained through a series of analyses of the standard gases with known amounts. The process for the sample analysis was generally similar to that of standard gas analysis. After the entire device was evacuated, all the four valves were closed, and the gold capsule was pierced. Gas components filled the space entrapped within valves A, B and D. Valve B was open to allow the components to be analyzed by the modified GC. The amounts of the gas components were determined from the values of FID and TCD responses and the equation aforementioned. As the total volume of gold, water and mineral oxidants of a large capsule ranged between 0.60 and 0.65 ml, about 2% of the volume of the effective space entrapped within valves A, B and D (30.6 ml), the corrected amounts of the gas components within the large capsule were about 2% lower than those calculated from the equation. A test with external standard gases indicated that this device had an accuracy of less than 0.5% in relative errors.

After the gas components entered the 6890N GC, valve B was closed. After GC analysis, the remaining gas components entrapped within valves A, B and D, with an amount about 80% of the initial value, were taken for gas chromatography–isotope ratio mass spectrometry (GC-IRMS) analysis using a specific syringe piercing through the septum (Fig. 1). This analysis was performed on a VG Isochrom II interfaced to an HP 5890 GC, which is located near this device. The HP 5890 GC was fitted with a Poraplot Q column (30 m × 0.32 mm i.d.). Helium was used as the carrier gas. The column head pressure was 8.5 psi.

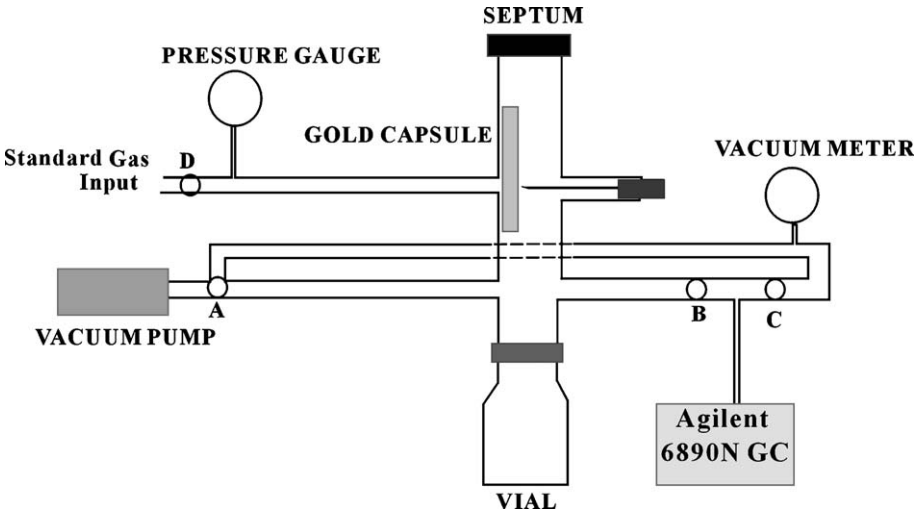

Fig. 1. Schema of the device for gas analysis.

The GC oven temperature was initially held at 40 °C for 3 min, ramped from 40 to 180 °C at 20 °C/min, and held at 180 °C for 5 min. The carbon isotopic value of CO_2 reference gas was calibrated by NBS 22 oil as a reference material using element analysis (Thermo Quest Flash EA 1112 Series), combined with isotope ratio mass spectrum (Delta Plus XL). Carbon isotope ratios for individual gaseous hydrocarbons were calculated using CO_2 as a reference gas that was automatically introduced into the IRMS at the beginning and end of each analysis. In addition, a standard mixture of gaseous hydrocarbons (C_1–C_4), with known isotope compositions calibrated by our laboratory, was used daily to test the performance of the instrument. Replicate analyses of this mixture show that the standard deviation for each compound is less than 0.3‰.

The procedure for the analysis of the large pyrolysates was as follows. The capsule was frozen in liquid nitrogen for more than 5 min, and then it was cut swiftly into several pieces in a vial, which contained about 3 ml pentane with 0.050 mg deuterated *n*-C_{24} (internal standard). Following five ultrasonic treatments with 5 min each cycle, the pentane solution was analyzed by GC and GC-MS.

3. Results

3.1. Chemical and isotopic compositions of kukersite kerogen pyrolysates

The chemical and isotopic compositions of gaseous pyrolysates within the nine selected small capsules are similar (Tables 1 and 2). The averaged amounts of methane, ethane and propane are 10.05, 3.31 and 1.30 mmol/g TOC, respectively. The averaged amounts of CO_2 and H_2S are 2.70 and 0.68 mmol/g TOC, respectively. The averaged $\delta^{13}C$ values for methane, ethane, propane and CO_2 are −42.0‰, −30.8‰, −20.5‰ and −33.8‰, respectively.

Table 2
Carbon isotopic compositions $\delta^{13}C$(‰) for gas components in the selected nine small capsules

	$C_1(\delta^{13}C‰)$	$C_2(\delta^{13}C‰)$	$C_3(\delta^{13}C‰)$	$CO_2(\delta^{13}C‰)$
1	−42.3	−31.1	−20.7	−33.7
2	−42.1	−30.5	−20.0	−34.0
3	−42.3	−30.8	−20.1	−34.2
4	−42.4	−31.0	−20.0	−33.7
5	−42.1	−31.0	−20.3	−33.6
6	−41.5	−30.4	−21.1	−34.0
7	−41.7	−30.9	−20.5	−33.8
8	−41.8	−30.9	−20.4	−33.7
9	−41.7	−30.9	−21.0	−33.6
AV	−42.0	−30.8	−20.5	−33.8
σ	0.32	0.22	0.43	0.21

AV: averaged value; $\delta^{13}C$ value of the initial kerogen: −31.6‰; $\delta^{13}C$ value of the residue kerogen after pyrolysis experiment: −31.5‰.

The $\delta^{13}C$ values in the initial kukersite kerogen and kerogen residues upon pyrolysing are −31.6‰ and −31.5‰, respectively, suggesting no carbon isotopic fractionation for this kerogen during pyrolysing at 450 °C.

The large pyrolysates contain only some polynuclear aromatic compounds, i.e., naphthalene, methylnaphthalenes, phenanthrene, methylphenanthrenes and pyrene (Fig. 2).

3.2. Chemical compositions upon oxidation

The amounts of volatile components upon oxidation are shown in Table 3 and Fig. 3. In the experiment using hematite, the amount of methane varied slightly and irregularly, ranging from 9.41 to 11.02 mmol/g TOC (93.6–109.7% of the initial value). The amount of ethane decreased consistently to 3.03 (91.5% of the initial value), 2.94–3.07 (88.8–92.7% of the initial value), 2.82–2.97 (85.2–89.7% of the initial value) and 2.72–2.80 mmol/g

Table 1
Amount of gaseous components in the selected nine small capsules (mmol/g TOC)

	C_1H_4	C_2H_6	C_2H_4	C_3H_8	C_3H_6	*i*-C_4H_{10}	*n*-C_4H_{10}	*i*-C_5H_{12}	*n*-C_5H_{12}	H_2	CO_2	H_2S
	All in mmol/g TOC											
1	10.02	3.35	0.00092	1.38	0.00269	0.185	0.069	0.00487	0.00420	0.24	2.57	0.67
2	9.66	3.39	0.00088	1.38	0.00264	0.178	0.065	0.00482	0.00407	0.25	2.62	0.70
3	9.96	3.33	0.00095	1.29	0.00271	0.182	0.066	0.00475	0.00400	0.24	2.62	0.69
4	10.04	3.26	0.00092	1.33	0.00267	0.176	0.064	0.00447	0.00373	0.25	2.61	0.68
5	9.87	3.26	0.00085	1.22	0.00207	0.141	0.041	0.00364	0.00319	0.17	2.78	0.66
6	9.91	3.16	0.00082	1.21	0.00204	0.144	0.045	0.00345	0.00278	0.18	2.63	0.65
7	10.16	3.25	0.00083	1.48	0.00205	0.189	0.093	0.00561	0.00448	0.29	2.73	0.68
8	10.56	3.42	0.00075	1.22	0.00209	0.141	0.035	0.00365	0.00327	0.33	2.86	0.69
9	10.31	3.33	0.00082	1.19	0.00205	0.136	0.034	0.00347	0.00317	0.33	2.84	0.68
AV	10.05	3.31	0.00086	1.30	0.00233	0.164	0.057	0.00430	0.00365	0.25	2.70	0.68
σ	0.25	0.08	0.00006	0.09	0.00031	0.022	0.018	0.00073	0.00054	0.05	0.10	0.01

AV: averaged value.

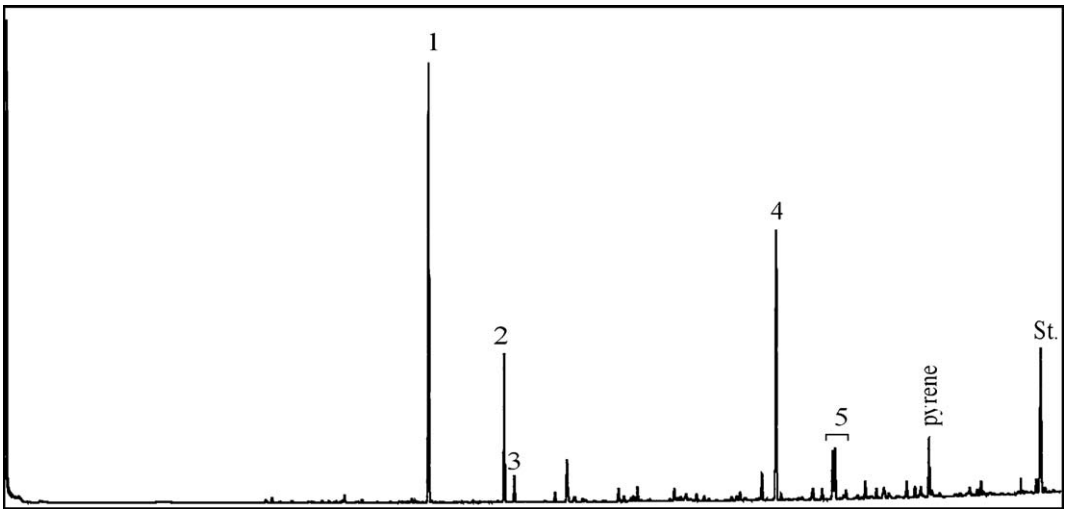

Fig. 2. Gas chromatograms of the large hydrocarbons (total pentane extracts): (1) naphthalene; (2) 2-methylnaphthalene; (3) 1-methylnaphthalene; (4) phenanthrene; (5) methylphenanthrenes; St.: internal standard deuterated n-C_{24}. Gas chromatography was performed on a HP6890 GC fitted with a 50-m × 0.32-mm i.d. column coated with a 0.40-μm film of CP-Sil 5CB, employing nitrogen as carrier gas. The oven temperature was programmed as follows: 40 °C for 5 min, raised from 40 °C to 290 °C at 4 °C/min, and then held at 290 °C for 45 min.

TOC (82.2–84.6% of the initial value) at 72, 144, 216 and 288 h, respectively. The amount of propane decreased at a relatively higher rate to 1.18 (90.7% of the initial value), 0.87–1.00 (66.9–76.9% of the initial value), 0.77–0.85 (59.2–65.4% of the initial value) and 0.71–0.73 mmol/g TOC (54.6–56.1% of the initial value) at 72, 144, 216 and 288 h, respectively. The amounts of butanes and pentanes decreased substantially at 72 h and then remained largely unchanged with further increased heating time. In addition, the reduction rate of isobutane and isopentane was substantially higher than that of the corresponding n-butane and n-pentane. Although the initial ratios of i-C_4/n-C_4 and i-C_5/n-C_5 are very high, 2.860 and 1.178, respectively, they were generally much less than 1 upon oxidation for 72–288 h (Table 3 and Fig. 4). Gas dryness value (C_1/C_{1-4} ratio) increased from the initial value of 0.675 to 0.699 at 72 h, to 0.729–0.734 at 144 h, and then decreased slightly to 0.710–0.722 at 216 h, and finally increased again to 0.739–0.740 at 288 h (Table 3, Fig. 5a). The amount of CO_2 increased substantially to 6.82 mmol/g TOC (2.53 times of the initial value) at 72 h and then varied slightly and irregularly with increasing heating time (Table 3). The ratio of $CO_2/(CO_2+\sum C_nH_{2n+2})$ increased from the initial value 0.154 to 0.324 at 72 h, then decreased slightly to 0.296–309 at 144 h, and increased again to 0.313–0.324 at 216 h, and finally, to 0.345–350 at 288 h (Fig. 5b). The amounts of H_2 and H_2S decreased rapidly to the levels below the detection limits at 72 h (Table 3).

For the experiment using $MgSO_4$ (magnesium sulfate heptahydrate), the amount of methane remained unchanged (98.7–100.6% of the initial value) at 72 h, increased substantially to 12.61–13.44 mmol/g TOC (125.5–133.7% of the initial value) at 144 h and maintained at this level with increasing heating time. The amount of ethane decreased slowly to 3.07–3.08 mmol/g TOC (92.7–93.1% of the initial value) at 72 h, and then decreased rapidly to 0.389–0.509 (11.8–15.4% of the initial value), 0.032–0.038 (1.00–1.11% of the initial value) and 0.007 mmol/g TOC (0.21% of the initial value) at 144, 216 and 288 h, respectively. The amount of propane decreased rapidly to 0.412–0.452 mmol/g TOC (31.7–34.8% of the initial value) at 72 h and to 0.007–0.023 mmol/g TOC (0.54–1.77% of the initial value) at 144 h, and then maintained this level with increasing heating time. The amounts of butanes and pentanes decreased rapidly to a very low level at 72 h and maintained at this level with increasing heating time. The reduction rate of isobutane and isopentane was also substantially higher than that of the corresponding n-butane and n-pentane, and the ratios of i-C_4/n-C_4 and i-C_5/n-C_5 were generally much less than 1 upon oxidation for 72–216 h (Fig. 4). C_1/C_{1-4} ratio increased slowly from the initial value of 0.675 to 0.737–0.743 at 72 h, and then increased rapidly to 0.961–0.970, 0.966 and 0.999 at 144, 216 and 288 h, respectively (Fig. 5a). The amount of H_2 was below the detection level during oxidation. The amount of CO_2 remained unchanged at 72 h and increased consistently with increasing heating time, from 2.64 mmol/g TOC at 72 h to 7.73 mmol/g TOC at 288 h (Table 3). The ratio of $CO_2/(CO_2+\sum C_nH_{2n+2})$ increased consistently from the initial value of 0.154 to 0.365 at 288 h (Fig. 5b).

Table 3
Residual amounts of gaseous components after oxidation experiments

	C_1H_4	C_2H_6	C_2H_4	C_3H_8	C_3H_6	*i*-C_4H_{10}	*n*-C_4H_{10}	*i*-C_5H_{12}	*n*-C_5H_{12}	H_2	CO_2	H_2S	C_1/C_{1-4}	C_2H_4/C_2H_6	C_3H_6/C_3H_8	*i*-C_4/*n*-C_4	*i*-C_5/*n*-C_5
	All in mmol/g TOC																
Initial	10.05	3.31	0.00086	1.30	0.00233	0.163	0.057	0.00430	0.00365	0.25	2.70	0.68	0.675	0.00026	0.00179	2.860	1.178
HEM																	
72 h	9.94	3.03	0.00062	1.18	0.00133	0.025	0.042	0.00170	0.00453	BD	6.82	BD	0.699	0.00020	0.00113	0.595	0.375
144 h-1	10.76	3.00	0.00052	0.94	0.00145	0.020	0.036	0.00126	0.00401	BD	6.36	BD	0.729	0.00017	0.00154	0.556	0.314
144 h-2	11.02	2.94	0.00037	1.00	0.00107	0.017	0.045	0.00132	0.00566	BD	6.71	BD	0.734	0.00013	0.00107	0.378	0.233
144 h-3	10.83	3.07	0.00056	0.87	0.00137	0.027	0.043	0.00165	0.00557	BD	6.23	BD	0.730	0.00018	0.00157	0.628	0.296
216 h-1	9.61	2.85	0.00042	0.81	0.00081	0.023	0.038	0.00139	0.00333	BD	6.09	BD	0.721	0.00015	0.00100	0.605	0.417
216 h-2	9.73	2.82	0.00040	0.85	0.00101	0.029	0.050	0.00190	0.00431	BD	6.47	BD	0.722	0.00014	0.00119	0.580	0.441
216 h-3	9.41	2.97	0.00039	0.77	0.00092	0.038	0.057	0.00205	0.00417	BD	6.20	BD	0.710	0.00013	0.00119	0.667	0.492
288 h-1	9.96	2.72	0.00034	0.73	0.00064	0.025	0.033	0.00171	0.00364	BD	7.10	BD	0.739	0.00013	0.00088	0.758	0.470
288 h-2	10.05	2.80	0.00039	0.71	0.00085	0.009	0.017	0.00071	0.00236	BD	7.33	BD	0.740	0.00014	0.00120	0.529	0.301
SUL																	
72 h-1	9.92	3.08	BD	0.452	0.00021	0.0011	0.0077	0.00015	0.00045	BD	2.64	2.74	0.737	–	0.00046	0.143	0.333
72 h-2	10.11	3.07	BD	0.412	0.00019	0.0007	0.0067	0.00013	0.00043	BD	2.80	2.78	0.743	–	0.00046	0.104	0.302
144 h-1	13.44	0.427	BD	0.007	0.00003	0.0002	0.0003	0.00005	0.00007	BD	3.67	6.41	0.969	–	0.00429	0.667	0.714
144 h-2	12.61	0.389	BD	0.007	0.00003	0.0002	0.0003	0.00006	0.00007	BD	3.70	6.28	0.970	–	0.00429	0.667	0.857
144 h-3	13.22	0.509	BD	0.023	0.00003	0.0004	0.0008	0.00004	0.00007	BD	3.66	6.05	0.961	–	0.00130	0.500	0.571
216 h-1	12.89	0.035	0.00040	0.008	0.00016	0.0006	0.0018	0.00045	0.00076	BD	5.85	7.22	0.996	0.01143	0.02000	0.333	0.592
216 h-2	12.90	0.032	0.00042	0.013	0.00016	0.0006	0.0019	0.00047	0.00081	BD	5.90	6.67	0.996	0.01313	0.01231	0.316	0.580
216 h-3	12.48	0.038	0.00037	0.009	0.00016	0.0006	0.0018	0.00044	0.00078	BD	5.91	6.38	0.996	0.00974	0.01778	0.333	0.564
288 h	13.43	0.007	BD	0.001	BD	BD	BD	BD	BD	BD	7.73	7.19	0.999	–	0.00046		

HS																
72 h	9.90	3.13	0.00029	1.08	0.00103	0.0221	0.0402	0.00109	0.00389	BD	2.37	BD	0.698	0.000093	0.00095	0.550	0.280
144 h	10.27	2.99	0.00026	0.71	0.00061	0.0181	0.0183	0.00011	0.00206	BD	2.32	BD	0.733	0.000087	0.00086	0.989	0.053
216 h-1	9.10	2.78	0.00020	0.89	0.00076	0.0003	0.0322	0.00016	0.00210	BD	2.24	BD	0.711	0.000072	0.00085	0.009	0.076
216 h-2	9.60	2.87	0.00021	0.81	0.00076	0.0002	0.0264	0.00011	0.00177	BD	2.39	BD	0.721	0.000073	0.00094	0.008	0.062
288 h-1	9.70	2.78	0.00019	0.71	0.00067	0.0001	0.0175	0.00010	0.00138	BD	2.20	BD	0.734	0.000068	0.00094	0.006	0.072
288 h-2	9.38	2.56	0.00018	0.55	0.00061	0.0002	0.0128	0.00010	0.00096	BD	2.09	BD	0.750	0.000070	0.00111	0.016	0.104
*HEM**																	
72 h	0.0130	0.03195	BD	0.01080	0.000086	0.000145	0.00055	0.000038	0.000050	BD	3.61	BD	0.230	–	0.00796	0.264	0.760
144 h	0.0096	0.00813	BD	0.00457	0.000047	0.000177	0.00061	0.000125	0.000307	BD	1.10	0.0307	0.415	–	0.01028	0.290	0.407
216 h	0.0190	0.01187	BD	0.00396	0.000042	0.000125	0.00047	0.000120	0.000206	BD	2.73	0.0513	0.536	–	0.01061	0.266	0.583
*SUL**																	
72 h	0.0413	0.02820	BD	0.02533	BD	0.000846	0.00124	0.000518	0.000956	BD	0.31	0.0589	0.426	–	–	0.682	0.542
144 h	0.0368	0.02226	BD	0.01149	0.000038	0.000411	0.00111	0.000133	0.000338	BD	0.28	0.0542	0.510	–	0.00331	0.370	0.393
216 h	0.0304	0.00372	BD	0.00035	BD	0.000029	0.00006	0.000022	0.000039	BD	0.14	0.4076	0.880	–	–	0.483	0.564
*HS**																	
72 h	0.04343	0.04218	BD	0.03238	BD	0.00496	0.00545	0.00065	0.00117	BD	0.42	0.0556	0.338	–	–	0.910	0.556
144 h-1	0.02826	0.01570	BD	0.00636	BD	0.00004	0.00039	0.00005	0.00013	BD	0.23	0.0618	0.557	–	–	0.103	0.385
216 h-2	0.03053	0.01758	BD	0.00735	BD	BD	0.00051	0.00002	0.00011	BD	0.21	0.2360	0.545	–	–	–	0.182

Initial: averaged value in Table 1; HEM: Fe_2O_3 as oxidant; SUL: $MgSO_4 \cdot 7H_2O$ as oxidant; HS: $Fe_2O_3 + MgSO_4 \cdot 7H_2O$ (7:6 wt.) as oxidant; *In the absence of initial gas reactants; BD: below detection level.

The amount of H_2S increased rapidly from the initial value of 0.68 mmol/g TOC to 2.74–2.78 mmol/g TOC (4.03–4.09 times of the initial value) at 72 h, to 6.05–6.41 mmol/g TOC (8.90–9.43 times of the initial value) at 144 h, and maintained at this level with increasing heating time. The ratio of $H_2S/(H_2S+\sum C_nH_{2n+2})$ increased from the initial value of 0.044 to 0.169–0.170 at 72 h, to 0.305–0.326 at 144 h, and further increased slightly with increasing heating time (Fig. 5c).

During the experiment using the mixed oxidants (hematite+magnesium sulfate heptahydrate), the compositional variation trends of gas components were similar to the results from the experiment using hematite with increasing heating time except that the amount of CO_2 was substantially lower with the mixed oxidants than with hematite alone (Table 3, Figs. 3 and 5).

In the comparative experiments without initial gas reactants, the amounts of gas hydrocarbons produced ranged from less than 1% to 2% of those in the corresponding experiments with the initial gas reactants except that the amounts of C_{2-5} hydrocarbons were similar in the experiments using magnesium sulfate heptahydrate with and without the initial gas reactants at 216 h or longer time (Table 3).

3.3. Carbon isotope compositions after oxidation experiment

Carbon isotopic compositions of methane, ethane, propane and CO_2 are shown in Table 4 and Fig. 6. Carbon isotopic compositions for the other gas hydrocarbons were not obtained due to their low absolute amounts.

In the experiment using hematite, the $\delta^{13}C$ value for methane increased slightly and varied irregularly in the range −41.5‰ to −40.1‰ with increasing heating time. The $\delta^{13}C$ value for ethane increased slowly from an initial value of −30.8‰ to −30.7‰, −29.2‰ to −28.8‰, −28.2‰ to −27.8‰ and −28.2‰ at 72, 144, 216 and 288 h, respectively. The $\delta^{13}C$ value for propane increased more prominently from an initial value of −20.5‰ to −18.3‰, −16.7‰ to −16.3‰, −17.3‰ to −16.9‰ and −15.8‰ to −15.7‰ at 72, 144, 216 and 288 h, respectively. The $\delta^{13}C$ value for CO_2 increased by about +2‰ in comparison with the initial value, but it remained quite invariant with increasing heating time.

In the experiment using magnesium sulfate heptahydrate, the $\delta^{13}C$ value for methane increased from the initial −41.7‰ to −39.0 to −38.9‰ at 72 h and to −36.2‰ to −35.6‰ at 144 h, remained largely unchanged at 216 h, ranging between −36.3‰ and −35.6‰, and finally increased to −34.5‰ at 288 h. The $\delta^{13}C$ value for ethane increased relatively slowly from the initial of −30.8‰ to −28.6‰ to −27.9‰ at 72 h, rapidly to −8.5‰ to −8.0‰ at 144 h and to −7.0‰ to −6.4‰ at 216 h, consistent with the varying trend of oxidation extent with increasing heating time. The $\delta^{13}C$ value for CO_2 decreased by +1.5‰ to +4‰ in comparison with the initial value.

In the experiment using the mixed oxidants, the varying trends of $\delta^{13}C$ values for methane, ethane and propane were similar to those in the experiment using hematite with increasing heating time. However, the $\delta^{13}C$ value for CO_2 decreased by about +4‰ in comparison with the initial value, similar to the results from the experiment using the magnesium sulfate heptahydrate.

4. Discussions

4.1. Methane as one of the final products of C2+ oxidation

In the experiment using $MgSO_4$, the amount of methane increased substantially at 144 h or with longer heating time (Table 3, Fig. 3a). This result clearly indicates that methane is one of the final products of C_2–C_5 hydrocarbon oxidation, as suggested by Seewald [21]. For example, the amount of methane was increased by about 3.39 mmol/g TOC, while that of C_2–C_5 hydrocarbons was decreased by about 4.5 mmol/g TOC at 144 h (144 h−1, Table 3). The oxidation of 1 mmol of C_2–C_5 hydrocarbons appeared to yield 1 mmol of methane. However, the amounts of C_2–C_5 alkanes decreased significantly (about 1.25 mol/g TOC in total) while the amount of methane even decreased slightly at 72 h (Table 3, Fig. 3a). This phenomenon can be interpreted as follows. The oxidation of C_2–C_5 alkanes was completed by a series of reactions. At the early stage, in addition to CO_2, only intermediate components, i.e., alcohols, ketones and organic acids, were produced [21], which were not analyzed in the present study. The rapid increase in the amount of methane after 72 h can be attributed to two causes: (1) the intermediate compounds produced prior to 72 h were finally transformed into CH_4 and oxidized into CO_2, and (2) the TSR accelerated as the reaction was progressing, as discussed later. The amount of methane was dependent on the rates of the two reactions, i.e., methane was oxidized to form CO_2 and at the same time was constantly produced from oxidation of C_2–C_5 alkanes. In the experiments using hematite and mixed oxidants, the amount of methane remained largely unchanged, indicating that the oxidation rate was similar to the generation rate (Table 3, Fig. 3a). As a result, the ratio of C_1/C_{1-4} increased with increasing heating time (Fig. 5a).

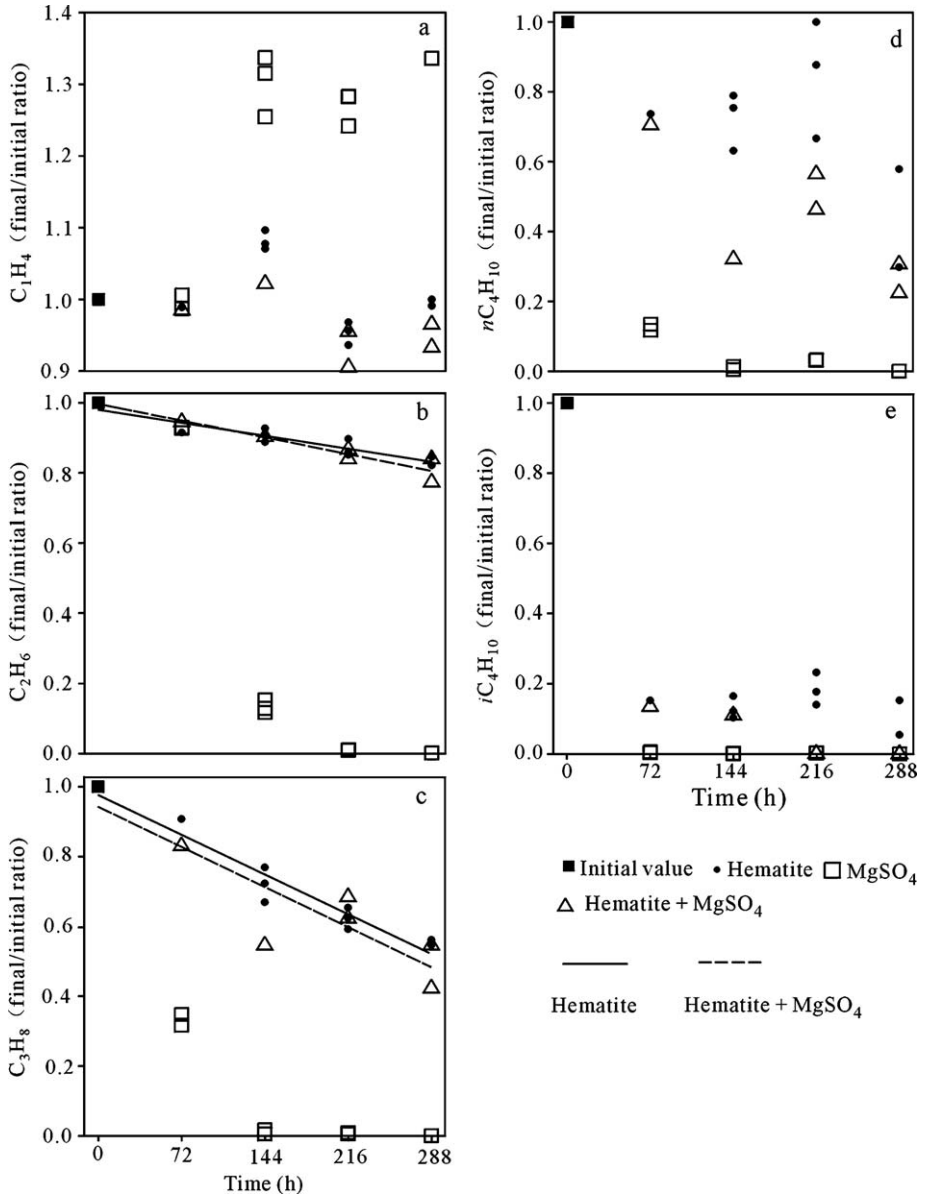

Fig. 3. Diagrams of heating time versus the amounts of C_1–C_4 alkanes.

4.2. Reaction rates

For all experiments using hematite, $MgSO_4$ and both, the oxidation rate of C_2–C_5 alkanes obviously increased with increasing carbon number in hydrocarbons and was higher for *i*-butane and *i*-pentane than for *n*-butane and *n*-pentane (Table 3 and Figs. 3 and 4). It can also be estimated that the oxidation rate of methane was the lowest even if the amount of methane generated from the oxidation of other alkanes was considered. Otherwise, the amount of methane would decrease substantially with increasing heating time because the initial ratio of $C_1/\sum C_{1-4}$ was 67.5 mol%. Oxidation rates of C_2–C_5 alkanes were substantially higher in the experiment using $MgSO_4$ than using hematite and the mixed oxidants (Table 3, Fig. 3). In contrast, the oxidation rate of methane relative to C_2–C_5 alkanes was opposite (Table 3, Fig. 3). It is noteworthy that the variation trends for gas hydrocarbons both in the amounts and carbon isotopic compositions were similar between the two experiments using hematite and the mixed oxidants (Tables 3 and 4, Figs. 3, 5a and 6)). This result demonstrates that gas alkanes mainly reacted with hematite rather than with $MgSO_4$ in the experiment

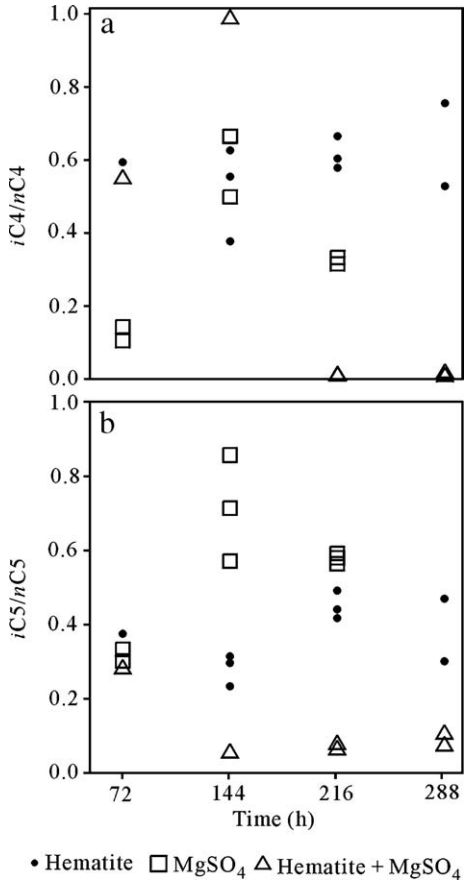

Fig. 4. Diagrams of heating time versus i-C_4/n-C_4 and i-C_5/n-C_5 ratios.

using the mixed oxidants. It suggests that the reaction between sulfates and gas hydrocarbons can be substantially influenced by other factors in addition to temperature.

Previous experimental studies on the oxidation of organic matter by aqueous sulfates demonstrated that TSR rate is extremely slow when H_2S is not present and increases with increasing partial pressure of H_2S [28,30,31]. In the present study, the oxidation rate of ethane was relatively low within 0–72 h in the experiment using $MgSO_4$, comparable to that in the experiments using hematite and the mixed oxidants, indicating a relatively low TSR rate (Table 3 and Fig. 3b). However, it increased substantially in the experiment using $MgSO_4$ after 72 h, indicating a high TSR rate (Fig. 3b). The different TSR rates during the experiment using $MgSO_4$ before and after 72 h could be accounted for by H_2S concentrations. In our experiment, the initial gas components contained a minor amount of H_2S (Table 1). Therefore, TSR started and proceeded slowly at the beginning and then accelerated with increasing amount of H_2S in the experiment using $MgSO_4$. Similarly, the extremely low TSR rate in the experiment using the mixed oxidants could be accounted for by the absence of H_2S. During this experiment, the initial H_2S preferentially reacted with hematite and precipitated as a result, resulting in the amount of H_2S below the detection level (Table 3). Therefore, TSR proceeded at an unnoticeable rate in the experiment using the mixed oxidants. This result implies that Fe-bearing minerals (i.e., hematite,

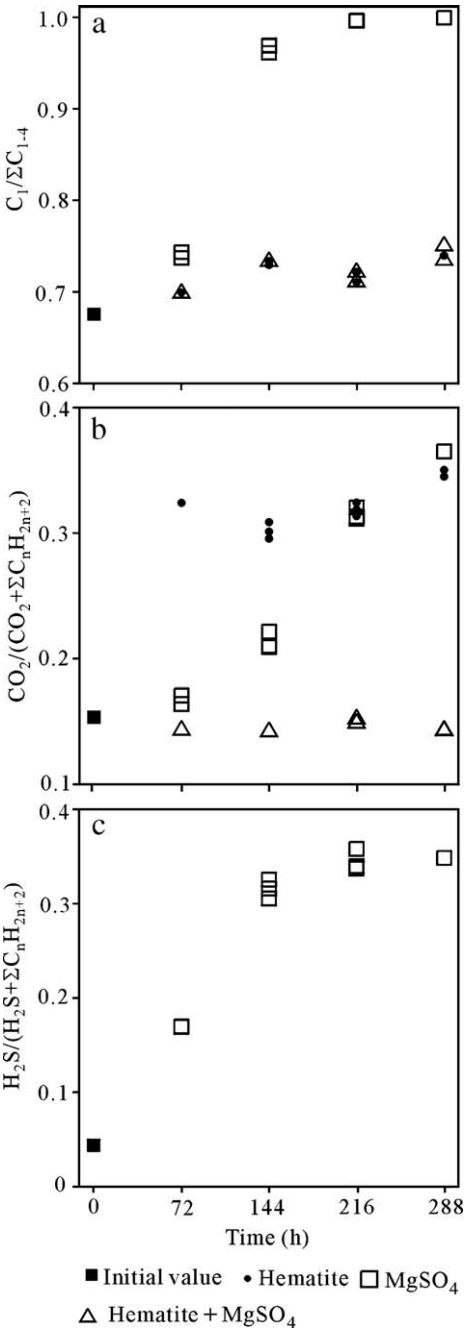

Fig. 5. Diagrams for the ratios of $C_1/\sum C_{1-4}$, $CO_2/(CO_2+\sum C_nH_{2n+2})$ and $H_2S/(H_2S+\sum C_nH_{2n+2})$ versus heating time.

Table 4
Carbon isotopic compositions $\delta^{13}C$(‰) for gas components

	CH_4	C_2H_6	C_3H_8	CO_2	α_{C2}	α_{C3}
Initial	−42.0	−30.8	−20.5	−33.8		
HEM						
72 h	−40.8	−30.7	−18.3	−31.7	1.0011	1.0249
144 h-1	−40.1	−29.2	−16.7	−31.6	1.0175	1.0126
144 h-2	−40.2	−28.8	−16.3	−31.7	1.0183	1.0173
144 h-3	−40.2	−29.1	−16.6	−31.4	1.0247	1.0104
216 h-1	−40.1	−27.8	−16.9	−32.0	1.0211	1.0081
216 h-2	−40.2	−27.8	−17.2	−32.0	1.0199	1.0084
216 h-3	−40.6	−28.2	−17.3	−32.1	1.0254	1.0066
288 h-1	−41.5	−28.5	−15.7	−31.5	1.0123	1.0088
288 h-2	−40.8	−28.5	−15.8	−31.4	1.0146	1.0082
SUL						
72 h-1	−38.9	−28.6	na	−36.8	1.0334	–
72 h-2	−39.0	−27.9	na	−36.9	1.0413	–
144 h-1	−36.2	−8.4	na	−37.4	1.0113	–
144 h-2	−35.6	−8.0	na	−37.1	1.0110	–
144 h-3	−36.0	−8.5	na	−36.8	1.0123	–
216 h-1	−36.3	−6.4	na	−35.4	1.0055	–
216 h-2	−35.6	−6.6	na	−35.4	1.0053	–
216 h-3	−35.8	−7.0	na	−34.9	1.0055	–
288 h	−34.5	na	na	−35.7	–	–
HS						
72 h	−41.4	−30.0	−20.5	−38.8	1.0157	1.0007
144 h	−41.0	−28.2	−18.5	−37.0	1.0272	1.0036
216 h-1	−40.2	−28.4	−18.1	−37.2	1.0144	1.0069
216 h-2	−39.9	−28.3	−18.1	−37.3	1.0188	1.0054
288 h-1	−40.3	−28.0	−14.2	−37.1	1.0172	1.0110
288 h-2	−40.5	−28.4	−15.2	−37.7	1.0100	1.0065

Initial: averaged value in Table 2; HEM: Fe_2O_3 as oxidant; SUL: $MgSO_4 \cdot 7H_2O$ as oxidant; HS: $Fe_2O_3 + MgSO_4 \cdot 7H_2O$ (7:6 wt.) as oxidant Sample; α_{C2}: kinetic isotope effect ($^{12}k/^{13}k$) for C_2H_6; α_{C3}: kinetic isotope effect ($^{12}k/^{13}k$) for C_3H_8; Both α_{C2} and α_{C3} are calculated based on Rayleigh equation (from Rooney et al. [40]): $(1/\alpha - 1)\ln f = \ln((10^{-3}\delta_f + 1)/(10^{-3}\delta_i + 1))$, f = final amount/initial amount of C_2H_6 or C_3H_8, δ_f and δ_i: final and initial values of $\delta^{13}C$; na: not measured due to low absolute amount.

magnetite, siderite, Fe-bearing clays, etc.) may inhibit TSR starting and proceeding by precipitating H_2S in natural systems. Machel mentioned a number of factors that may influence TSR rate and temperature range in sedimentary basin [9]. He also mentioned that iron sulfides are rare by-products of TSR in sour gas reservoirs and ascribed this result to no Fe available in the reservoir rocks [9]. Our interpretation of this phenomenon is that TSR did not occur in reservoir rocks that contained abundant Fe-bearing minerals, and even if iron sulfides occurred in sour gas reservoirs in some cases, they formed prior to TSR initiation, more likely during bacterial sulfate reduction.

Heydari suggested that during TSR anhydrite reacted with H_2S to produce S^0, which in turn reacted with CH_4 to generate more H_2S in a self-reinforcing cycle, based on his observations of TSR within Upper Jurassic Smackover Formation, Black Creek Field, Mississippi [6]. Worden et al. also demonstrated that the TSR is an autocatalytic process in their study of deep carbonate gas reservoirs within the Permian Khuff Formation, Abu Dhabi [16]. However, they ascribed this phenomenon mainly to the generation of a large amount of water during TSR [16]. TSR is not a pure gas–solid reaction but occurs between methane and anhydrite both dissolved in water [8,9,14,16]. The salinity of in situ

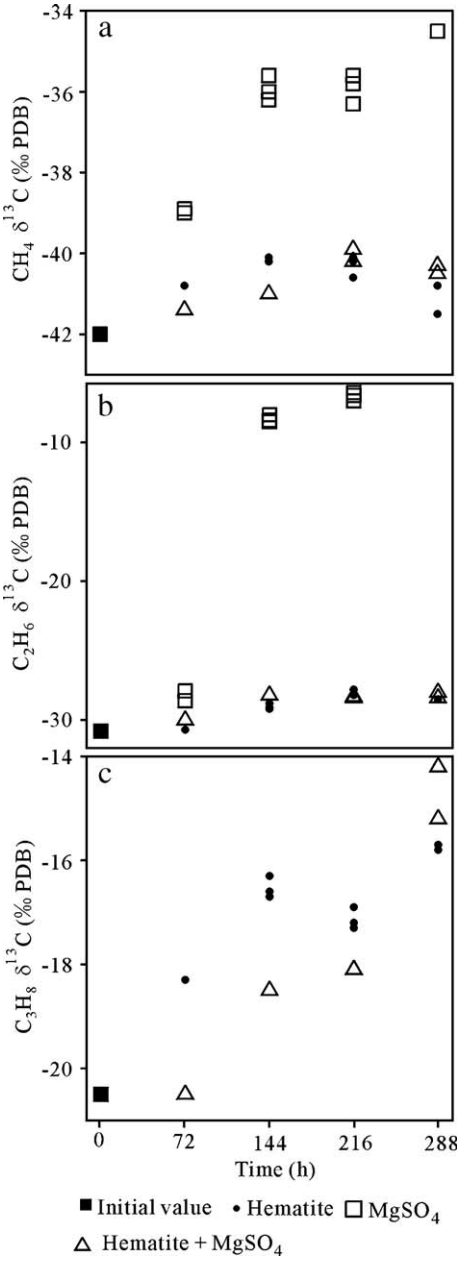

Fig. 6. Diagrams of heating time versus $\delta^{13}C$ values of methane, ethane and propane.

water decreases due to the addition of a large amount of water [16]. As a result, the solubility of methane and anhydrite increases [16]. Machel especially emphasized the importance of the wettability effect on TSR and concluded that TSR of solid sulfates is not possible in a diagenetic environment [9]. In the present study, the oxidation rates of gas alkanes were slightly higher in the experiment using the mixed oxidants than hematite alone (Table 3 and Fig. 3). This result may be also ascribed to water generation due to dehydration of $MgSO_4{\cdot}7H_2O$ at 350 °C. An alternative interpretation is that the oxidation rates of gas alkanes by hematite may be enhanced by active aqueous sulfur in the experiment using the mixed oxidants [21].

4.3. Net mass balance reaction

Orr proposed a pair of reactions to account for the observed variation in chemistry and stable isotope composition of gases during TSR in the Big Horn Basin, USA [2,3]:

$$SO_{4\,(aq)}^{2-} + 3H_2S \rightarrow 4S + 2H_2O + 2OH^- \quad (1)$$

$$4S + 1.33(-CH_2-) + 2.66H_2O \rightarrow 4H_2S + 1.33CO_2 \quad (2)$$

This pair of reactions actually stemmed from the experimental work of Toland [31] and was supported by recent laboratory studies [28,30]. Worden and Smalley [13] emphasized the importance of direct reaction between gas hydrocarbons and dissolved sulfates, and proposed the following reactions:

$$CaSO_4 + CH_4 \rightarrow CaCO_3 + H_2S + H_2O \quad (3)$$

$$2CaSO_4 + C_2H_6 \rightarrow 2CaCO_3 + H_2S + S + 2H_2O \quad (4)$$

As mentioned previously, TSR did not occur in the experiment with the mixed oxidants. Therefore, reactions (3) and (4) are inconsistent with our experimental results. We believe that reactions (1) and (2) are generally appropriate to account for the results of our experiment using $MgSO_4$. Reaction (2) can be also written as

$$3S + (-CH_2-) + 2H_2O \rightarrow 3H_2S + CO_2 \quad (5)$$

For methane, the reaction can be written as

$$4S + CH_4 + 2H_2O \rightarrow CO_2 + 4H_2S \quad (6)$$

For ethane, propane and *i*-butane, however, the reaction equations in our experiment are somewhat different from Orr's and can be written as

$$3S + C_2H_6 + 2H_2O \rightarrow 3H_2S + CH_4 + CO_2 \quad (7)$$

$$6S + C_3H_8 + 4H_2O \rightarrow 6H_2S + CH_4 + 2CO_2 \quad (8)$$

$$9S + i\text{-}C_4H_{10} + 6H_2O \rightarrow 9H_2S + CH_4 + 3CO_2 \quad (9)$$

As demonstrated by Seewald, one *n*-butane molecule forms two acetic acid molecules during oxidative degradation, which may subsequently form two methane molecules via decarboxylation [21]. For *n*-butane, the reaction can be written as

$$5S + n\text{-}C_4H_{10} + 4H_2O \rightarrow 5H_2S + 2CH_4 + 2CO_2 \quad (10)$$

Reaction (6) proceeds substantially slower than do the other reactions. The reaction rate for the above reactions decreases in the sequence of reaction (9)> reaction (10)> reaction (8)> reaction (7)> reaction (6). Although the solid minerals were not analyzed after the oxidation experiment, it can be deduced that CO_2 could partly precipitate as $MgCO_3$ during the experiment under the consideration that the oxidation extent of C_{2+} components was substantially high while the amount of CO_2 and the ratio of $CO_2/(CO_2+\sum C_nH_{2n+2})$ were substantially low in this experiment, in comparison with the experiment using Fe_2O_3 at 72 h and 144 h (Table 3, Figs. 3 and 5b):

$$CO_2 + Mg^{2+} + 2OH^- \rightarrow MgCO_3 + H_2O \quad (11)$$

Reactions (6)–(10) suggest that the proportions of H_2S, CO_2 and H_2O produced during TSR vary substantially due to different gas hydrocarbon reactants. The net reactions for methane, ethane, propane and *n*-butane can be written as

$$SO_{4\,(aq)}^{2-} + Mg^{2+} + CH_4 \rightarrow MgCO_3 + H_2S + H_2O \quad (12)$$

$$3SO_{4\,(aq)}^{2-} + 3Mg^{2+} + 4C_2H_6 \rightarrow 3MgCO_3 + 4CH_4 + 3H_2S + CO_2 + H_2O \quad (13)$$

$$3SO_{4\,(aq)}^{2-} + 3Mg^{2+} + 2C_3H_8 \rightarrow 3MgCO_3 + 2CH_4 + 3H_2S + CO_2 + H_2O \quad (14)$$

$$5SO_{4\,(aq)}^{2-} + 5Mg^{2+} + 4n - C_4H_{10} + H_2O \rightarrow 5MgCO_3 + 8CH_4 + 5H_2S + 3CO_2 \quad (15)$$

For methane, no CO_2 is produced and H_2S and H_2O are produced in the ratio $H_2S/H_2O = 1:1$ via reaction (12). For ethane and propane, H_2S, CO_2 and H_2O are

produced in the proportion $H_2S/CO_2/H_2O = 3:1:1$ via reactions (13) and (14). However, for *n*-butane, water is consumed rather than generated, and H_2S and CO_2 are produced in the ratio $H_2S/CO_2 = 5:3$ via reaction (15). The critical difference between our observations and the previous studies is that we directly observed the substantial increase rather than the decrease in the amount of methane during TSR. This phenomenon has not been noticed in the previous studies of TSR [1–19].

Machel pointed out in a review paper that whether water is a volumetrically significant net reaction product cannot usually be ascertained in field studies [9]. Worden et al. concluded that a large amount of water was produced during TSR, based on fluid inclusion and isotopic data of TSR calcites of the Khuff Formation, Abu Dhabi [16]. However, Machel [10] and Machel et al. [11] provided strong evidence that no measurable amount of water was released during TSR in hydrocarbon reservoirs within the Devonian Nisku Formation of western Canada. Our view on this issue is that the amount of water produced during TSR is dependent on gas reactants, as shown in reactions (12)–(15). For gas reservoirs within Permian Khuff Formation, methane is the only available hydrocarbon for TSR due to extremely high dryness value (>0.95) at the beginning of TSR [13]. Therefore, a relatively large amount of water was produced via reaction (12). In contrast, for gas reservoirs within the Devonian Nisku Formation of western Canada, hydrocarbons with higher molecular weights are the dominant reactants [9–12]. As a result, no or only a small amount of water was generated via reactions (13)–(15) in these reservoirs.

In the experiments using hematite and the mixed oxidants, reactions between gas components and oxidants can be written as follows:

$$2H_2S + Fe_2O_3 \rightarrow FeS_2 + Fe^{2+} + 2OH^- + H_2O \quad (16)$$

$$CH_4 + 4Fe_2O_3 \rightarrow CO_2 + 6FeO + 2Fe^{2+} + 4OH^- \quad (17)$$

$$C_2H_6 + 3Fe_2O_3 \rightarrow CO_2 + CH_4 + 5FeO + Fe^{2+} + 2OH^- \quad (18)$$

$$C_3H_8 + 6Fe_2O_3 \rightarrow 2CO_2 + CH_4 + 10FeO + 2Fe^{2+} + 4OH^- \quad (19)$$

$$i\text{-}C_4H_{10} + 9Fe_2O_3 \rightarrow 3CO_2 + CH_4 + 15FeO + 3Fe^{2+} + 6OH^- \quad (20)$$

$$n\text{-}C_4H_{10} + 5Fe_2O_3 \rightarrow 2CO_2 + 2CH_4 + 9FeO + Fe^{2+} + 2OH^- \quad (21)$$

The result that the amount of CO_2 increased from the initial value of 2.70–6.82 mmol/g TOC at 72 h, but remained largely unchanged with increasing heating time using Fe_2O_3 demonstrates that $FeCO_3$ precipitation could occur significantly in this experiment after 72 h (Table 3):

$$CO_2 + Fe^{2+} + 2OH^- \rightarrow FeCO_3 + H_2O \quad (22)$$

Fe^{2+} and FeO occurred more likely in the form of Fe_3O_4, in addition to $FeCO_3$ in the reaction cell. Although the oxidation extent of C_{2+} components was slightly higher in the experiments using the mixed oxidants than using Fe_2O_3, the amount of CO_2 and the ratio of $CO_2/(CO_2 + \sum C_nH_{2n+2})$ remained virtually unchanged and were substantially lower in the former than in the latter. This result suggests that a large part of CO_2 was removed primarily as $MgSO_4$ precipitation via reaction (11) due to overwhelmingly high Mg^{2+} concentrations relative to Fe^{2+} concentrations in the experiment using the mixed oxidants.

It is noteworthy that the CO_2 $\delta^{13}C$ value in the experiment using the mixed oxidants was similar to that in the experiment using $MgSO_4$, but about 5–7‰ higher than that in the experiment using hematite (Table 4). The CO_2 $\delta^{13}C$ value after oxidation was determined by three factors, the initial $\delta^{13}C$ value of CO_2, the $\delta^{13}C$ value of CO_2 generated during oxidation and the carbon isotopic fractionation due to precipitation as carbonate (i.e., $MgCO_3$ and $FeCO_3$). As discussed earlier, gas alkanes mainly reacted with hematite rather than $MgSO_4$ in the experiment using the mixed oxidants, and the oxidation extent of gas alkanes in this experiment was similar to that using hematite while significantly lower than that in the experiment using $MgSO_4$ (Table 3 and Figs. 3, 5a and 6). Therefore, the difference of CO_2 $\delta^{13}C$ values among the three experiments can be mainly ascribed to the precipitation of carbonates. The CO_2 $\delta^{13}C$ value also demonstrates that a significant amount of CO_2 was removed as $MgCO_3$ precipitation in the experiment using the mixed oxidants, just as in the experiment using $MgSO_4$.

4.4. Pyrobitumen as a reactant

In the comparative experiment using hematite, CO_2 was produced in the amount of 1.10–3.61 mmol/g TOC during 72–216 h. In addition, trace amounts of gas hydrocarbons were also generated, e.g., $0.96–1.30 \times 10^{-2}$ mmol/g TOC of methane (Table 3). These results suggest that the reaction between pyrobitumen and hematite proceeded at a considerable rate in the absence of the initial gas reactants. In the comparative experiment using the mixed oxidants, 0.21–0.42 mmol/g TOC of CO_2 was produced, substantially lower than those generated in the comparative experiment using hematite alone. However, the amounts of gas

hydrocarbons released from the former, e.g., 2.82–4.34×10^{-2} mmol/g TOC of methane, were substantially higher than from the latter (Table 3). As discussed previously, hematite appears slightly more effective in reacting with gas hydrocarbons in the experiment using the mixed oxidants than using hematite alone. It can be estimated that the oxidation extent of pyrobitumen in the comparative experiment using the mixed oxidants was at least as high as in the comparative experiment using hematite alone. The lower amount of CO_2 in the former resulted from the precipitation of $MgCO_3$. In the comparative experiment using $MgSO_4$, the amounts of CO_2 and gas hydrocarbons released were similar to those in the comparative experiment using the mixed oxidants. This result may suggest a similar oxidation extent of pyrobitumen between these two experiments.

The oxidation of pyrobitumen by Fe^{3+}-bearing minerals may be insignificant in sedimentary basins because these minerals are generally relatively rare in reservoir rocks, e.g., typically 1–2 wt.% of Fe_2O_3 in red sandstones [22]. If this red sandstone is charged by oil, Fe_2O_3 will preferentially react with liquid hydrocarbons. It consumes 30 g of Fe_2O_3 to oxidize 1 g of alkanes (–CH_2–) completely into CO_2. If the red sandstone is charged by gas hydrocarbons, no pyrobitumen will be formed. However, the oxidation of pyrobitumen during TSR may be important. The reservoir rocks of TSR generally contain abundant sulfates (anhydrite), which cannot be used up. Therefore, there is the possibility that sulfates react with pyrobitumen. It can be speculated that this reaction may result in the formation of elemental sulfur due to the scarcity of hydrogen in pyrobitumen. As described by Heydari and Heydari and Moore [5,6], the reservoir rocks within Upper Jurassic Smackover Formation, Black Creek field, were charged with oil. With increasing burial depth and temperature, this oil was converted into gas hydrocarbons and pyrobitumen. Within gas window, TSR started and proceeded. The most important processes and products of gas window diagenesis are (1) dissolution and calcitization of anhydrite, (2) post-bitumen calcite cementation, and (3) formation of elemental sulfur [5,6]. In the present study, only trace amounts of H_2S (0.05–0.41 mmol/g TOC) were produced from the reaction between pyrobitumen and $MgSO_4$ (Table 3). This result is likely to indicate that SO_4^{2-} was mainly reduced into elemental sulfur, rather than suggesting a low oxidation extent of pyrobitumen. Machel noted that TSR elemental sulfur sometimes occurs as minute crystals embedded in solid bitumen [9]. During TSR, pyrobitumen is not only a product, but also a reactant. The reaction between the oxidants and pyrobitumen more likely occurred in the solid pyrobitumen phase and the contact zone between the aqueous phase and pyrobitumen. The dissolved oxidants along with water can be partitioned into pyrobitumen. In contrast, the reaction between gaseous hydrocarbons and mineral oxidants mainly occurred in the aqueous phase.

4.5. Ratios of i-butane/n-butane and i-pentane/n-pentane

Previous pyrolysis studies suggested that, in petroleum formation processes, *n*-alkanes were formed through free radical reactions, whereas the branched isoalkanes arose from two processes: (1) free radical cracking of branched fragments of kerogen and bitumens, and (2) carbonium ion reaction of α-olefins with protons which were enhanced in acidic conditions [44–46]. In other words, isoalkanes/*n*-alkanes ratio was controlled by two factors: (1) kerogen nature, i.e., relative content of straight chain fragments to branched fragments, and (2) the result of competition between free radical reaction of *n*-alkenes to form *n*-alkanes and the carbonium ion reaction of *n*-alkenes with protons to form isoalkanes. As introduced by Thompson and Creath [47], the analyses of several hundred natural gases and approximately 100 crude oils, covering many of the producing areas in the U.S. and Canada and including Miocene to Cambrian production, indicate that $i\text{-}C_4/n\text{-}C_4$ ratio is usually of the order of 0.5 and rarely >1.0, and that $i\text{-}C_5/n\text{-}C_5$ ratio is usually of the order 1.0, and rarely >2.0 (highest observed: 3.5). These data indicate that commercial oils and gases are formed mostly via free radical reactions and occasionally via carbonium ion reactions.

In the present study, the initial values of $i\text{-}C_4/n\text{-}C_4$ and $i\text{-}C_5/n\text{-}C_5$ ratios were 2.860 and 1.178, respectively. These values became substantially lower than 1 in all three experiments upon oxidation (Table 3 and Fig. 4). This result provides an additional interpretation of the low values of these two ratios for natural hydrocarbon reservoirs.

4.6. Carbon isotopic fractionation factor

The carbon isotopic fractionation factor α (k^{12}/k^{13}) for ethane, calculated with the Rayleigh equation [40], decreases with increasing heating time in the experiment using $MgSO_4$, i.e., 1.0334–1.0413 within 0–72 h, 1.0110–1.0123 within 0–144 h and 1.0053–1.0055 within 0–216 h (Table 4). These data represent average $\dot{\alpha}$ values within the time intervals. As discussed earlier, ethane oxidation accelerated with increasing heating time in this experiment (Fig. 3b). At 72 h, the amount of ethane decreased to the level 93% of the initial value. At 144 h, it decreased to the level 14.4% of the amount at

72 h. At 216 h, it decreased to the level only 7.92% of the amount at 144 h (Table 3). These results clearly show that factor α decreases with increasing oxidation rate. As most of the ethane (79.5% of the initial amount) was removed between 72 and 144 h (Table 3 and Fig. 3b), the range of 1.0110–1.0123 could be the representative of factor α values for ethane in this experiment. In contrast, the values of factor α for ethane and propane did not exhibit a clear variation trend with increasing heating time in the experiments using Fe_2O_3 and the mixed oxidants (Table 4). This is because that the oxidation rates of ethane and propane appeared constant in these two experiments (Fig. 3b and c). The average values of factor α were 1.0192 for ethane and 1.0100 for propane in the experiment using hematite, and 1.0172 for ethane and 1.0067 for propane in the experiment using the mixed oxidants. The values of factor α for ethane and propane at 72 h deviated substantially from the other data and, therefore, were excluded from the average values. This result can be ascribed to the fact that only small amounts of ethane and propane were oxidized, and therefore, the analytic errors could significantly influence the values of factor α. The slightly higher values of factor α in the experiment using hematite may also be attributed to the slightly lower reaction rate in this experiment, in comparison with those in the experiment using the mixed oxidants (Fig. 3b and c).

Kiyosu and Krouse [27] found that the value of factor α for methane decreased with increasing temperature and obtained the following relationships between factor α and temperature through abiogenic oxidation of methane:

$$10^3(\alpha-1) = 2.93 \times 10^6/T^2 + 8.11 \text{ (cupric oxide)}$$

$$10^3(\alpha-1) = 7.44 \times 10^6/T^2 + 6.56 \text{ (hematite)}.$$

Factor α of methane varied from 1.0202 at 450 °C to 1.0127 at 650 °C in the experiment using hematite and from 1.0153 at 370 °C to 1.0106 at 590 °C in the experiment using cupric oxide [27]. It would have been about 1.0481 for hematite and 1.0245 for cupric oxide if temperature was extrapolated to 150 °C based on the above equations. If we consider that reaction rate increases with increasing temperature, our result that factor α decreased with increasing oxidation rate is consistent with this previous study [27].

Previous studies have documented that TSR rate increased with TSR proceeding in natural reservoirs [6,16]. The oxidation rate of gas hydrocarbons by Fe^{3+}-bearing minerals could also vary with temperature (100–200 °C), catalytic conditions and pH and E_h values. Therefore, factor α could vary significantly during abiogenic oxidation in natural reservoirs. However, because temperatures in natural reservoirs are substantially lower than our experimental temperature, it can be deduced that the factor α value would be higher in natural reservoirs than those obtained from our experiments, i.e., higher than 1.0110–1.0123 for ethane in natural TSR reservoirs, and higher than 1.0192 and

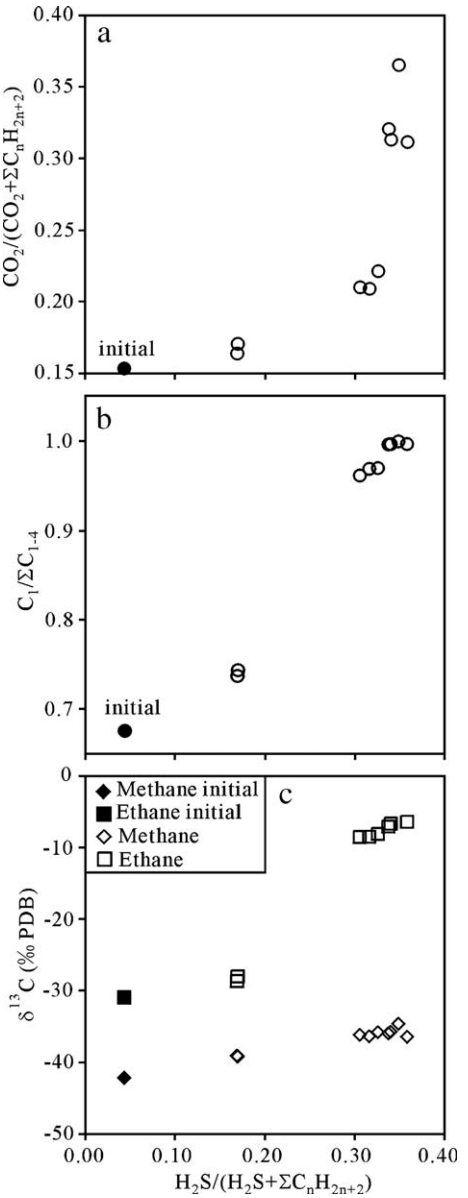

Fig. 7. Diagrams of $H_2S/(H_2S+\sum C_nH_{2n+2})$ ratio versus the ratios of $CO_2/(CO_2+\sum C_nH_{2n+2})$ and $C_1/\sum C_{1-4}$, and $\delta^{13}C$ values of methane and ethane in the experiment using $MgSO_4$.

1.0100, respectively, for ethane and propane during abiogenic oxidation by hematite in natural non TSR reservoirs.

4.7. Comparison with natural TSR process

In the present study, ratios of $H_2S/(H_2S+\sum C_{2n}H_{2n+2})$, $CO_2/(CO_2+\sum C_{2n}H_{2n+2})$ and $C_1/\sum C_{1-4}$ and $\delta^{13}C$ values for gas hydrocarbons increased substantially and consistently with proceeding TSR (Figs. 5 and 7). To date, the case studies of TSR in natural environments have focused on the following formations and regions: (1) the Jurassic Smackover Formation of the United States [1–6]; (2) the Devonian Nisku Formation in western Canada [10–12]; (3) Devonian and Mississippian sour gas fields in western Canada [7]; (4) the Permian Khuff Formation of Abu Dhabi [13–16]; (5) Triassic sour gas reservoirs in Sichuan Basin, China [17,19]; and (6) the Cambro-Ordovician formations in Central Tarim, China [18]. All these studies demonstrated that the amount of H_2S, or the ratio of $H_2S/(H_2S+\sum C_{2n}H_{2n+2})$, increased substantially and consistently with the extent of TSR [1–19]. However, $C_1/\sum C_{1-4}$ ratio and $\delta^{13}C$ values of gas hydrocarbons responded differently to TSR of reservoirs in different regions (Table 5) [1,7,13,19]. For reservoirs within Smackover and Norphlet formations in southwestern Alabama, as documented by Claypool and Mancini [1], both $C_1/\sum C_{1-5}$ ratio and methane $\delta^{13}C$ value did not increase with increasing amount of H_2S. As these reservoirs contained relatively high amount of liquid oil, sulfates preferentially reacted with long-chain alkanes (C_{15+}) during TSR [1]. In contrast, for reservoirs within the Devonian and Mississippian formations in western Canada, the Permian Khuff Formation of Abu Dhabi, and Triassic formations in Sichuan Basin, China, the ratios of $C_1/\sum C_{1-4}$ and $CO_2/(CO_2+\sum C_{2n}H_{2n+2})$, and $\delta^{13}C$ values of gas hydrocarbons increased substantially with increasing TSR extent [7,13–17,19], consistent with the result of our experiment (Table 5). Just as in our experiment, the reservoirs in these regions contain no or very little C_{6+} hydrocarbons, and sulfates only react with gas hydrocarbons (C_{1-5}). Although the variation trends are similar, the variation extents are substantially different for $\delta^{13}C$ values of gas hydrocarbons during TSR in our experiments and the three cases documented by Krous et al. [7], Worden et al. [13–16], and Cai et al. [19]. As illustrated in Table 5, the variation of methane $\delta^{13}C$ value during TSR is up to +22‰ in the case documented by Worden et al. [13–16], up to +5‰ in the cases reported by Krous et al. [7], up to +2.9‰ in the case reported by Cai et al. [19] and up to +7.5‰ in our experiment. The variation of ethane $\delta^{13}C$ value during TSR is up to +10‰ in the case reported by Krous et al. [7], up to +0.9‰ (only two samples) in the case reported by Cai et al. [19] and up to +24.4‰ in our experiment. Although the carbon isotopic fractionation factor α in natural environments could be higher than in our experiment as discussed earlier, the magnitude of $\delta^{13}C$ value increase for gas hydrocarbons during TSR decreases in the following order: the case reported by Worden [13–16] > our TSR experiment > the case reported by Krous et al. [7] > the case reported by Cai et

Table 5
Comparison with natural TSR data

	Claypool and Mancini [1]		Krouse et al. [7]		Worden et al. [13–16]		Cai et al. [19]		The present study	
	Pre-TSR	TSR	Pre-TSR	TSR	Pre-TSR	TSR	Pre-TSR	TSR	Pre-TSR	TSR
H_2S (%)	0.0–0.2	4.6–23.9	<2	Up to 30	<5	Up to 50	0.0	Up to 17.4	3.72	Up to 27.76
$H_2S/(H_2S+\sum C_nH_{2n+2})$					<0.1	Up to 0.5	0	Up to 0.18	0.04	Up to 0.358
CO_2 (%)	1.6–4.9	2.4–50.1					<1	Up to 10.4	14.78	Up to 27.26
$CO_2/(CO_2+\sum C_nH_{2n+2})$					0.02–0.1	0.30	0.0	Up to 0.12	0.153	Up to 0.365
$CO_2/(CO_2+\sum nC_nH_{2n+2})$			0.06	Up to 0.15					0.112	Up to 0.365
C_1/C_{1-4}	0.52–0.93	0.63–0.80			0.90–0.95	Up to 1.0	0.994	Up to 0.999	0.675	Up to 0.999
CH_4 $\delta^{13}C$ (‰)	−40.8 to −38.0	−45.6 to −41.6	Up to +5 increase during TSR		−45 to −40	Up to −23	−32.4	Up to −29.5	−42.0	Up to −34.5
C_2H_6 $\delta^{13}C$ (‰)			Up to +10 increase during TSR				−33.8	−32.9	−30.8	Up to −6.4

al. [19]. This is consistent with that of TSR extent, which was estimated from the abundance of H_2S or the ratio of $H_2S/(H_2S+\sum C_nH_{2n+2})$ (Table 5). In general, a large increase in $\delta^{13}C$ value of gas hydrocarbons, together with a high ratio of $H_2S/(H_2S+\sum C_nH_{2n+2})$, indicates a high TSR extent for a TSR gas reservoir. By contrast, a small increase in $\delta^{13}C$ value of gas hydrocarbons, together with a strikingly high ratio of $H_2S/(H_2S+\sum C_nH_{2n+2})$, more likely indicates a mixing process, either by H_2S from a reservoir with severe TSR or by gas hydrocarbons with light or mild TSR. The mixing of gases with different TSR extents may occur in geological processes and even during gas production and sampling processes.

4.8. Oxidation of gas hydrocarbons in non-TSR reservoirs

Oxidation of gas hydrocarbons through Fe^{+3}-bearing mineral reduction was generally ignored in the previous studies [32–41]. However, Seewald emphasized that the hydrolytic disproportionation reactions and oxidative degradation of hydrocarbons by Fe-bearing minerals may widely occur and be important in sedimentary basins and further suggested that the aqueous oxidation may be an effective mechanism to remove the C_{2+} components of wet gas and to generate methane, which could resolve the issue regarding the origin of thermogenic dry gas [20,21]. Based on the results of our experiments, we believe that the extent of oxidation of C_{2+} hydrocarbons is commonly low (<30–50%) and occasionally high (>80–90%) in natural non-TSR gas reservoirs. The carbon isotope data can be used to constrain the oxidation extents of gas hydrocarbons. In our experiment using hematite, the increases of $\delta^{13}C$ values for methane, ethane and propane were up to +1.9‰, +3.0‰ and +4.7‰, respectively, whereas the oxidation extents of ethane and propane were up to 17.8% and 45.4%, respectively. In the experiment using the mixed oxidants, the increases of $\delta^{13}C$ values for methane, ethane and propane were up to +1.8‰, +2.8‰ and +6.2‰, respectively, while the oxidation extents of ethane and propane were up to 22.7% and 57.7% respectively. Moreover, as discussed earlier, carbon isotopic fractionation would be severe due to the low temperature in natural reservoirs, in comparison with the result in our experiment. The oxidation extent of methane was difficult to determine because methane was formed from the oxidation of C_{2+} alkanes. However, it is certain that the oxidation extent of methane was lower than that of ethane. If the oxidation extents of C_{2+} alkanes are too high (>80–90%), the $\delta^{13}C$ values for these alkanes would be extraordinarily high (>−15‰), which was rarely reported in sedimentary basins [32–41]. In addition, mineral oxidants preferentially react with alkanes with relatively high molecular weight (C_{6+}); thus, oxidation of gas hydrocarbons (C_{1-5}) is insignificant in oil reservoirs. Nevertheless, although at a low extent, oxidation of gas hydrocarbons by Fe^{+3}-bearing minerals can still significantly change the chemical and isotopic compositions of gas hydrocarbons and blur the other effects, i.e., sources and thermal maturation [32–41]. The oxidative effect needs to be considered seriously for the non-TSR gas reservoirs.

5. Conclusions

In the present study, the variations of proportion and carbon isotope compositions of gas hydrocarbons upon oxidation by hematite, $MgSO_4$ and both were demonstrated through a unique two-step experimental approach. The variation trends for the gas components with increasing oxidation time are outlined as follows:

(1) The amount of methane remained almost unchanged in the experiments using hematite and the mixed oxidants, whereas it increased substantially after 72 h in the experiment using $MgSO_4$, indicating that methane was one of the final products from C_{2+} oxidation.
(2) The amounts of C_2–C_5 hydrocarbons decreased consistently and more rapidly in the experiment using $MgSO_4$ than in those using hematite and the mixed oxidants.
(3) The oxidation rates of gas hydrocarbons increased with increasing carbon number of hydrocarbons.
(4) The oxidation rates of *i*-butane and *i*-pentane were substantially higher than those of the corresponding *n*-butane and *n*-pentane.
(5) The amount of H_2S increased substantially in the experiment using $MgSO_4$, whereas it was below the detection level in the experiments using hematite and the mixed oxidants.
(6) The $\delta^{13}C$ values of C_1–C_5 hydrocarbons became less negative and the isotopic fractionation extent increased with increasing carbon number of hydrocarbons and oxidation extent.
(7) Carbon isotopic fractionation factor α (k^{12}/k^{13}) decreased with increasing oxidation rate of gas hydrocarbons.
(8) TSR was inhibited by hematite which precipitated H_2S as pyrite in the experiment using the mixed oxidants.

The results of our experiments imply that TSR may not occur in reservoir rocks containing abundant Fe-bearing minerals other than ferric sulfides. During TSR, the amount

of water produced may be closely dependent on the hydrocarbon reactants. If methane is the only reactant, a relatively large amount of water will be produced. In contrast, if hydrocarbons with higher molecular weight (C_{2+}) are present, no or very little water will be produced. The oxidation extent of C_{2+} hydrocarbons by Fe^{3+}-bearing minerals may be generally low (<30–50%) in natural non-TSR reservoirs, constrained from carbon isotope data. However, a low extent of oxidation can significantly change the chemical and isotopic compositions of gas hydrocarbons and blur the other effects, i.e., sources and thermal maturation. Therefore, the oxidative effect needs to be considered seriously for the non-TSR gas reservoirs.

Acknowledgements

This study was supported by the National Natural Science Foundation of China (Grant No. 40473033), the State 973 Program of China (Grant No. 2005CB422102) and Chinese Academy of Sciences (GIGCX-04-08). We thank Dr A. Prinzhofer and an anonymous reviewer for their constructive reviews of our paper.

References

[1] G.E. Claypool, E.A. Mancini, Geochemical relationships of petroleum in Mesozoic reservoirs to carbonate source rocks of Jurassic Smackover Formation, southwestern Alabama, AAPG Bull. 73 (1989) 904–924.

[2] W.L. Orr, Changes in sulfur content and isotopic ratios of sulfur during petroleum maturation—study of Big Horn Basin Paleozoic oils, AAPG Bull. 58 (1974) 2295–2318.

[3] W.L. Orr, Geologic and geochemical controls on the distribution of hydrogen sulfide in natural gas, in: R. Campos, J. Goni (Eds.), Advances in Organic Geochemistry 1975, Madrid, Spain, Enadimsa, 1977, pp. 571–597.

[4] R. Sassen, Geochemical and carbon isotopic studies of crude oil destruction, bitumen precipitation, and sulfate reduction in the deep Smackover Formation, Org. Geochem. 12 (1988) 351–361.

[5] E. Heydari, C.H. Moore, Burial diagenesis and thermochemical sulfate reduction, Smackover Formation, southeast Mississippi salt basin, Geology 17 (1989) 1080–1084.

[6] E. Heydari, The role of burial diagenesis in hydrocarbon destruction and H_2S accumulation, Upper Jurassic Smackover Formation, Black Creek Field, Mississippi, AAPG Bull. 81 (1997) 26–45.

[7] H.R. Krous, C.A. Viau, L.S. Eliuk, A. Ueda, S. Halas, Chemical and isotopic evidence of thermal-chemical sulphate reduction by light hydrocarbon gases in deep carbonate reservoirs, Nature 333 (1988) 415–419.

[8] H.G. Machel, H.R. Krouse, R. Sassen, Products and distinguishing criteria of bacterial and thermochemical sulfate reduction, Appl. Geochem. 10 (1995) 373–385.

[9] H.G. Machel, Bacterial and thermochemical sulfate reduction in diagenetic settings—old and new insights, Sediment. Geol. 140 (2001) 143–175.

[10] H.G. Machel, Saddle dolomite as a by-product of chemical compaction and thermochemical sulfate reduction, Geology 15 (1987) 936–940.

[11] H.G. Machel, H.R. Krouse, L.R. Riciputi, D.R. Cole, Devonian Nisku sour gas play, Canada: a unique natural laboratory for study of thermochemical sulfate reduction, in: M.A. Vairavamurthy, M.A.A. Scoonen (Eds.), Geocchemical Transformations of Sedimentary Sulfur, ACS Symposium Series, vol. 612, 1995, pp. 439–454.

[12] B.K. Manzano, M.G. Fowler, H.G. Machel, The influence of thermochemical sulfate reduction on hydrocarbon composition in Nisku reservoirs, Brazeau River area, Alberta, Canada, Org. Geochem. 27 (1997) 507–521.

[13] R.H. Worden, P.C. Smalley, H_2S-producing reactions in deep carbonate gas reservoirs: Khuff Formation, Abu Dhabi, Chem. Geol. 133 (1996) 157–171.

[14] R.H. Worden, P.C. Smalley, M.M. Cross, The influence of rock fabric and mineralogy upon thermochemical sulfate reduction: Khuff Formation, Abu Dhabi, J. Sediment. Res. 70 (2000) 1218–1229.

[15] R.H. Worden, P.C. Smalley, N.H. Oxtoby, Gas souring by thermochemical sulfate reduction at 140 °C, AAPG Bull. 79 (1995) 854–863.

[16] R.H. Worden, P.C. Smalley, N.H. Oxtoby, The effects of thermal sulfate reduction upon formation water salinity and oxygen isotopes in carbonate gas reservoirs, Geochim. Cosmochim. Acta 60 (1996) 3925–3931.

[17] C. Cai, R.H. Worden, S.H. Bottrell, L. Wang, C. Yang, Thermochemical sulphate reduction and the generation of hydrogen sulphide and thiols (mercaptants) in Triassic carbonate reservoirs from the Sichuan Basin, China, Chem. Geol. 202 (2003) 39–57.

[18] C. Cai, W. Hu, R.H. Worden, Thermochemical sulphate reduction in Cambro-Ordovician carbonates in Central Tarim, Mar. Pet. Geol. 18 (2001) 729–741.

[19] C. Cai, Z. Xie, R.H. Worden, G. Hu, L. Wang, H. He, Methane-dominated thermochemical sulphate reduction in the Triassic Feixianguan Formation East Sichuan Basin, China: towards prediction of fatal H_2S concentrations, Mar. Pet. Geol. 21 (2004) 1265–1279.

[20] J.S. Seewald, Organic–inorganic interactions in petroleum-producing sedimentary basins, Nature 426 (2003) 327–333.

[21] J.S. Seewald, Aqueous geochemistry of low molecular weight hydrocarbons at elevated temperatures and pressures: constraints from mineral buffered laboratory experiments, Geochim. Cosmochim. Acta 65 (2001) 1641–1664.

[22] R.C. Surdam, Z.S. Jiao, D.B. MacGowan, Redox reactions involving hydrocarbons and mineral oxidants: a mechanism for significant porosity enhancement in sandstones, AAPG Bull. 77 (1993) 1509–1518.

[23] R.C. Surdam, L/J. Crossey, E.S. Hagen, Heasler, Organic–inorganic interactions and sandstone diagenesis, AAPG Bull. 73 (1989) 1–32.

[24] Y.K. Kharaka, W.W. Carothers, R.J. Rosenbbauer, Thermal decarboxylation of acetic acid; implications for the origin of natural gas, Geochim. Cosmochim. Acta 47 (1983) 397–402.

[25] P.D. Lundegard, L.S. Land, Carbon dioxide and organic acids, the role in porosity enhancement and cementation, Paleocene of the Texas Gulf Coast, in: D. Gautier (Ed.), Role of Organic Matter in Sediment Diagenesis, Society of Economic Paleontologists and Mineralogists Publication, vol. 38, 1986, pp. 129–146.

[26] S.G. Franks, R.W. Forester, Relationships amongst secondary porosity, pore fluid chemistry and carbon dioxide, Texas Gulf Coast, in: D. MacDonald, R. Sudam (Eds.), Clastic Diagenesis, AAPG Memoir, vol. 37, 1986, pp. 63–80.

[27] Y. Kiyosu, H.R. Krouse, Carbon isotope effect during abiogenic oxidation of methane, Earth Planet. Sci. Lett. 95 (1989) 302–306.
[28] Y. Kiyosu, H.R. Krouse, Thermochemical reduction and sulfur behavior of sulfate by acetic acid in the presence of native sulfur, Geochem. J. 27 (1993) 49–57.
[29] M.M. Cross, D.A.C. Manning, S.H. Bottrell, R.H. Worden, Thermchemical sulphate reduction (TSR): experimental determination of reaction kinetics and implications of the observed reaction kinetics and implications of the observed reaction rates for petroleum reservoirs, Org. Geochem. 35 (2004) 393–404.
[30] M.B. Goldhaber, W.L. Orr, Kinetic controls on thermochemical sulfate reduction as a source of sedimentary H_2S, in: M.A. Vainravamurth, M.A.A. Schoonen (Eds.), Geochemical Transformations of Sedimentary Sulfur, ACS Symposium Series, vol. 612, 1995, pp. 412–625.
[31] W.G. Toland, Oxidation of organic compounds with aqueous sulfate, J. Am. Chem. Soc. 82 (1960) 1911–1916.
[32] W.J. Stahl, B.D. Carey Jr., Source rock identification by isotopic analyses of natural gases from fields in the Val Verde and the Delaware Basin, West Texas, Chem. Geol. 16 (1975) 257–267.
[33] M. Schoell, The hydrogen and carbon isotopic composition of methane from natural gases of various origins, Geochim. Cosmochim. Acta 44 (1980) 649–661.
[34] U. Berner, E. Faber, Empirical carbon isotope/maturity relationships for gases from algal kerogens and terrigenous organic matter, based on dry, open-system pyrolysis, Org. Geochem. (1996) 947–955.
[35] U. Berner, E. Faber, G. Scheeder, D. Panten, Primary cracking of algal and landplant kerogens: kinetic models of isotope variations in methane, ethane, and propane, Chem. Geol. 126 (1995) 233–245.
[36] B. Cramer, B.M. Krooss, R. Littke, Modeling isotope fractionation during primary cracking of natural gas: a reactive kinetic approach, Chem. Geol. 149 (1998) 235–250.
[37] E.M. Galimov, Sources and mechanisms of formation of gaseous hydrocarbons in sedimentary rocks, in: M. Schoell (Ed.), Origins of Methane in the Earth, Chem. Geol., vol. 71, 1988, pp. 77–99.
[38] A.T. James, Correlation of reservoired gases using the carbon isotopic compositions of wet gas components, AAPG Bull. 74 (1990) 1441–1458.
[39] A.A. Prinzhofer, A.Y. Huc, Genetic and post-genetic molecular and isotopic fractionations in natural gases, Chem. Geol. 126 (1995) 281–290.
[40] M.A. Rooney, G.E. Claypool, H.M. Chung, Modeling thermogenic gas generation using carbon isotope ratios of natural gas hydrocarbons, Chem. Geol. 126 (1995) 219–232.
[41] Y. Tang, J.K. Perry, P.D. Jenden, M. Schoell, Mathematical modeling of stable isotope ratios in natural gases, Geochim. Cosmochim. Acta 64 (2000) 2673–2687.
[42] S. Derenne, C. Largeau, E. Casadevall, J.S. Sinninghe Damste, E.W. Tegelaar, J.W. de Leeuw, Characterization of Estonian kukersite by spectroscopy and pyrolysis: evidence for abundant alkyl phenolic moieties in an Ordovician marine, type II/I kerogen, Org. Geochem. 16 (1990) 871–888.
[43] V. Salmon, S. Derenne, E. Lallier-Verges, C. Largeau, B. Beaudoin, Protection of organic matter by mineral matrix in a Cenomanian black shale, Org. Geochem. 31 (2000) 463–474.
[44] E. Eisma, J.W. Jurg, Fundamental aspects of the generation of petroleum, in: G. Eglinton, M.T.J. Murphy (Eds.), Organic Geochemistry, Methods and Results, Springer-Verlag, Berlin, 1969, pp. 675–698.
[45] W.R. Almon, W.D. Johns, Petroleum-forming reactions. The mechanism and rate of clay catalyzed fatty acid decarboxylation, in: R. Campos, J. Goni (Eds.), Advances in Organic Geochemistry 1975, Enadimsa, Madrid, 1977, pp. 157–172.
[46] Y.V. Kissin, Catagenesis and composition of petroleum: origin of *n*-alkanes and isoalkanes in petroleum crudes, Geochim. Coszmochim. Acta 51 (1987) 2445–2457.
[47] R.R. Thompson, W.B. Creath, Low molecular weight hydrocarbons in recent and fossil shells, Geochim. Cosmochim. Acta 30 (1966) 1137–1152.